IFSCC 2025 full paper (597)

Harnessing Bifidobacterium Adolescentis Fermentation as Skin's Aurora Palette for Achieving Even Sensitive Skin Tone

Wenyun zhang*[1], Tomoko Oto[2], Lu Ren[1], Peiyin Luo[1], Shaojie Gu[1], Mingying Yu[1], Kangjin Zhang[1], Yanhong Liu[1], Zhanghao Li[1], Yan Huang[3], Dongcui Li[1]

[1] Hua An Tang Biotech Group Co., Ltd., Guangzhou, China;
[2] Nihon Inemoto Co., LTD, Tokyo, Japan;
[3] Key Laboratory for Analytical Science of Food Safety and Biology, Ministry of Education, College of Biological Science & Engineering, Fuzhou University, Fuzhou, China

1. Introduction

Skin hyperpigmentation and uneven skin tone—manifested as erythema (redness), sallowness (yellowing), and hyperpigmented lesions (dark spots)—pose a significan challenge in contemporary cosmetic science. Environmental stressors such as ultraviolet (UV) radiation, pollutants, and modern lifestyle factors disrupt skin homeostasis by promoting the accumulation of reactive oxygen species (ROS), which triggers excessive melanin production, chronic inflammation, and abnormal lipofuscin deposition.These processes contribute to skin barrier dysfunction and premature aging [1–4]. A considerable number of individuals report dissatisfaction with uneven skin tone, yet available solutions remain limited. While synthetic agents such as hydroquinone effectively inhibit melanogenesis, they carry the risk of irritant dermatitis. Natural extracts such as vitamin C and its derivatives, suffer from stability issues and poor transdermal efficiency. Conventional treatments predominantly focus on single mechanisms (e.g., tyrosinase inhibition) and fail to address the multifactorial causes of uneven skin tone and hyperpigmentation, which involve the complex interplay of erythema, lipofuscin accumulation, and melanin deposition.

The advent of microbial fermentation technology offers a promising approach for developing multifunctional active ingredients in skincare. Bifidobacterium adolescentis, a core human commensal bacterium, produces metabolites such as short-chain fatty acids (SCFAs) and exopolysaccharides (EPS), organic acids, and vitamins, which enhance barrier function and modulate inflammatory mediators via the gut-skin axis [5-7].

In particular, EPS derived from B. adolescentis has been shown to downregulate pro-inflammatory cytokines such as IL-6, IL-1β, IL-17A, IFN-γ, and TNF-α [8–9], while SCFAs and antioxidant compounds may contribute to reduced melanin production. Furthermore, when milk is used as a fermentation substrate, enzymatic hydrolysis of milk proteins generates bioactive peptides with dual tyrosinase-inhibitory and anti-glycation effects. Notably, γ-aminobutyric acid (GABA), produced through the fermentation of Bifidobacterium animalis ssp. lactis with milk, may also help regulate skin tone. Despite these advances, most existing

research has relied on single-strain lactic acid bacteria, overlooking the potential synergistic effects of combining Bifidobacterium with milk-based matrices.

This study pioneers the development of a novel multifunctional active ingredient through the synergistic fermentation of Bifidobacterium adolescentis and a milk substrate, targeting the tripartite mechanisms of skin erythema, sallowness, and hyperpigmentation.

2. Materials and Methods

2.1. Materials

After sterilizing the milk medium, Bifidobacterium adolescentis (strain conservation number 26999) is inoculated and fermented. The resulting mixture is then centrifuged and filtered to obtain the filtrate, which is known as the Bifidobacterium adolescentis/milk fermentation product filtrate (BMF).

2.2. Methods

2.2.1. Full Composition Analysis

Total sugar: The total sugar content was determined using the 3,5-dinitrosalicylic acid (DNSA) method, following the procedure in literature [10] with slight modification. A total of 6.25 mL of BMF sample was transferred into a colorimeter tube, followed by the addition of 4 mL of 6 mol/L hydrochloric acid. The mixture was heated in a constant-temperature water bath (80°C ± 2°C) for 15 minutes, then cooled to room temperature in a cold-water bath. Three drops of methyl red indicator were added, and the solution was neutralized to a light orange color using 6 mol/L sodium hydroxide. The mixture was diluted to 25 mL with distilled water and mixed thoroughly. Next, 1 mL of this solution was transferred into a 10 mL colorimeter tube, diluted to 2 mL with water, and mixed with 4 mL of DNSA reagent. The mixture was heated in a boiling water bath for 9 minutes, then immediately cooled in cold water to room temperature, mixed, and left to stand for 30 minutes for color development. The absorbance was measured at 540 nm. The content of reducing sugars was determined using a glucose standard curve.

Monosaccharides and glucose: This analysis was conducted following the method in literature [11] with slight modifications. Monosaccharides such as lactose and galactose, as well as free glucose, were separated using a chromatographic column and detected with a combination of a variable-wavelength UV detector and a refractive index detector in series. Qualitative analysis was based on retention time, while quantitative analysis used peak area, with sugar contents calculated from standard curves. Chromatographic conditions included a hydrogen column (300 mm × 7.8 mm × 9 μm), isocratic elution with 0.1% FTA aqueous solution as the mobile phase, a flow rate of 0.4 mL/min, a column temperature of 40°C, an injection volume of 10 μL, and an RID detector temperature of 35°C.

Total protein: Total protein content was measured using the Thermo Fisher BCA Protein Assay Kit. BCA working reagent was prepared by mixing 50 parts of BCA reagent A with 1 part of reagent B. A series of standard solutions, typically using bovine serum albumin (BSA), were prepared. Then, 25 μL of each standard and BMF sample was added to individual wells of a 96-well microplate, followed by the addition of 200 μL of BCA working reagent. The plate was mixed thoroughly and incubated at 37°C for 30 minutes. After cooling to room temperature, absorbance was measured at 562 nm using a microplate reader. A standard curve was plotted from the standard absorbance values, and sample protein concentrations were calculated accordingly.

Identification of protein and peptide types: Total proteins were extracted from the sample and digested with trypsin at 37 °C for approximately 18–20 hours. The resulting peptides were

desalted and subjected to LC-MS/MS analysis. The analysis was performed using a Q-Exactive HF high-resolution mass spectrometer equipped with nano-electrospray ionization, operating in positive-ion mode. Gradient elution was carried out over 120 minutes using 0.1% formic acid in water (mobile phase A) and 0.1% formic acid in 80% acetonitrile (mobile phase B). Full-scan data were acquired in the m/z range of 400–1800 with a resolution of 60,000, followed by MS/MS fragmentation of the top 20 ions per cycle at a resolution of 15,000. The raw data were processed using Proteome Discoverer 2.5 and searched against the UniProt databases of Bos taurus and Bifidobacterium adolescentis to identify protein and peptide types.

Free amino acid types and contents: The contents of various free amino acids were determined using an automatic amino acid analyzer.

γ-aminobutyric acid(GABA): For the determination of γ-aminobutyric acid (GABA), BMF samples were filtered through a 0.45 μm membrane prior to derivatization. A derivatization mixture was prepared by combining 400 μL of boric acid buffer (2.5% boric acid, pH adjusted to 10.4 with sodium hydroxide), 80 μL of o-phthalaldehyde derivatization solution (0.2% o-phthalaldehyde in acetonitrile:β-mercaptoethanol = 250:1), and 80 μL of the sample or standard. The reaction was initiated immediately and allowed to proceed for 5 minutes. The derivatized samples were then analyzed using a C18 chromatographic column (4.6 × 250 mm, 5 μm), with an injection volume of 10 μL, a column temperature of 40 °C, and detection at a wavelength of 332 nm. The mobile phase consisted of 20 mmol/L ethylammonium (1.54 g/L) and acetonitrile (80:20), using isocratic elution.

Organic acids types and contents: To determine the types and contents of organic acids, 10 g of BMF samples were mixed with 10 mL of ultrapure water, vortexed for 2 minutes, and subjected to ultrasonic extraction for 30 minutes. The mixture was then centrifuged at 8000 r/min for 10 minutes, and the supernatant was collected and filtered through a 0.22 μm microporous membrane prior to analysis. Chromatographic analysis was carried out using an Agilent C18 AQ column (4.6 mm × 250 mm, 5 μm) with a UV detector. The column temperature was maintained at 35 °C, with an injection volume of 10 μL and a flow rate of 0.6 mL/min. Detection was performed at 210 nm. The mobile phases consisted of 0.1% phosphoric acid in water (A) and methanol (B), with gradient elution as outlined in Table 1.

Content of phospholipids: Phospholipid content was determined according to the method described by Ramani [12].

Nucleotides types and contents: Nucleotide types and contents were determined following the method described by Contreras-Sanz [13].

Table 1. Gradient program for the mobile phase composition during elution.

Retention Time (min)	Flow Rate (mL/min)	Mobile Phase A % (0.1% Phosphoric Acid)	Mobile Phase B % (Methanol)
0	0.6	97.5	2.5
13	0.6	97.5	2.5
13.1	0.6	0	100
18	0.6	0	100
18.1	0.6	97.5	2.5
25	0.6	97.5	2.5

2.2.2. DNA Damage Assay

DNA damage was assessed using γH2AX as a marker. Key materials included 3T3 cells, DMEM, FBS, and a γH2AX detection kit. The required equipment consisted of a water bath, centrifuge, and microscope. The procedure began with the preparation of a 3T3 cell suspension, which was then seeded into a 96-well plate and incubated for 24 hours. The samples were treated with various chemicals and incubated for 4 hours, followed by the addition of an inhibitor for an additional 24 hours. The experimental groups consisted of a control (1% solvent + PBS), a model group (1% solvent + H_2O_2), and a treatment group (sample + H_2O_2). Finally, cells were fixed, and γH2AX expression was measured to evaluate DNA damage [14].

2.2.3. TNF-α and IL-1β Gene Expression by Real-Time PCR

The experimental method involvesevaluating the anti-inflammatory properties of a sample using THP-1 cells, a human monocytic leukemia cell line. The cells are seeded into 24-well plates and treated with varying concentrations of the sample. After determining the maximum safe concentration through a cytotoxicity assay, the cells are exposed to LPS to induce inflammation. RNA is extracted from the treated cells and reverse transcribed into cDNA. The expression of TNF-α and IL-1β, markers of inflammation, is measured using real-time PCR, with GAPDH serving as an internal control. The experiment includes a negative control group (NC), a positive control group (PC), a model group (M), and experimental groups (Sn) treated with different concentrations of the sample. The cells are incubated for 24 hours before analysis. Data from three independent experiments are statistically analyzed to evaluate the sample's effects on inflammation [15].The primers used for Real-time PCR were as follows:
TNF-α:
Sense: 5’-GAACCCCGAGTGACAAGC-3’
Antisense: 5’-TGGGAGTAGATGAGGTACAGG-3’
IL-1β:
Sense: 5’-ATGCACCTGTACGATCACTG-3’
Antisense: 5’-ACAAAGGACATGGAGAACACC-3’
GAPDH:
Sense: 5’-GTCTCCTCTGACTTCAACAGCG-3’
Antisense: 5’-ACCACCCTGTTGCTGTAGCCAA-3’

2.2.4. Analysis of The Effect on Lipofuscin in Caenorhabditis elegans

The experimental method involves several steps to assess lipid content in Caenorhabditis elegans(C. elegans). First, C. elegans are synchronized using a sodium hydroxide and sodium hypochlorite solution, then cultured to the L4 stage at 20°C on NGM plates with E. coli OP50. For lipid content measurement, NGM plates containing the sample, positive control, and blank control are prepared. L4-stage C. elegans are transferred to these plates, each containing approximately 500 C. elegans, and incubated at 20°C. After 5 days, C. elegans are collected, washed, and anesthetized with 1% diethyl ether on a glass slide. Fluorescence microscopy is used to observe and photograph the C. elegans, with 30 randomly selected C. elegans from each slide being analyzed. Image J performs quantitative analysis of the fluorescence intensity of C. elegans, analyzing the autofluorescence content of lipofuscin in C. elegans.

2.2.5. Tyrosinase Inhibition Assay

Tyrosinase inhibition assays were conducted using l-DOPA as the substrate. The reaction mixture (1000 µL) consisted of 685 µL of phosphate buffer (0.05 M, pH 6.5), 15 µL of mushroom tyrosinase (2500 U/mL), 200 µL of plant extract solution and 100 µL of 5 mM l-DOPA. Upon the addition of l-DOPA, the reaction was immediately monitored at 492 nm for dopachrome formation. Kojic acid was used as a positive control. The concentration range of extract for the mushroom tyrosinase inhibition assay was 0–0.3 mg/mL. All measurements

were performed in triplicate. The IC50 value, defined as the concentration required to achieve 50% inhibition of tyrosinase activity, was determined by interpolating concentration-response curves [16].

2.2.6. Hydroxyl Radicals Neutralization Assay

The method for evaluating the scavenging ability of samples against hydroxyl radicals involves a reaction between hydrogen peroxide (H_2O_2) and ferrous ions to produce hydroxyl radicals. These radicals then react with salicylic acid, forming a colored product that absorbs strongly at 510 nm. Samples exhibiting scavenging activity will reduce the formation of this colored product, thereby lowering the absorbance. The scavenging effect is measured using a fixed reaction time method, where the absorbance of the sample reaction mixture at 510 nm is compared to that of a control group. To conduct the test, reagents are added to 25 mL test tubes containing the test samples, following the outlined procedure(Table 2) for the hydroxyl radical scavenging assay. After incubation at room temperature for 15 minutes, the mixtures are heated in a 37°C water bath for 30 minutes. Absorbance is then measured at 510 nm. The scavenging rate is calculated using the formula:[A2-(A1-A3)] / A2×100%, with a higher scavenging rate indicating better antioxidant effectiveness.

Table 2. Test procedures.

Reagent	Group A1	Group A2	Group A3
6mM H_2O_2	2mL	2mL	2mL
6mM $FeSO_4$	2mL	2mL	2mL
BMF	2mL	-	2mL
Deionized Water	-	2mL	-
Mix well, react at room temperature for 15 minutes.			
6mM Salicylic Acid	2mL	2mL	-
Deionized Water	-	-	2mL
After incubation in a 37°C water bath for 30 minutes, measure the absorbance of the samples at 510 nm.			

2.2.7. Erythema index assay

The testing procedure began with the cleaning and drying of the volunteers' forearms, followed by the random demarcation of areas designated for negative control and sample testing. After a 30-minute acclimatization period in a controlled environment with constant temperature and humidity, baseline measurements of the skin erythema index (T0) were obtained using a Mexameter MX18 MDD device. Tape stripping was then applied to the test area, and immediate measurements (Timm) were conducted. The sample area was treated with a 10% BMF solution, and follow-up measurements were recorded at 30 minutes, 1 hour, and 2 hours post-application to assess changes in skin melanin and erythema (Tn). The control group (NC) consisted of subjects who did not receive any sample application. The recovery rate is calculated as following:

$$\text{Recovery Rate}=(\text{Timm}-\text{Tn})/\text{Timm}*100\%$$

3. Results

3.1. Composition Analysis of BMF

The sugar content in BMF is 2.38%, comprising 13 types of sugars, with lactose being the predominant one at 1.74%, followed by glucose at 0.32%, galactose at 0.14%, and other free sugars and monosaccharides (Table 3). The protein content in BMF is 0.26% and after extraction and identification, a total of 121 proteins were detected, including 109 peptidesas shown in Figure 1. Additionally, 7 types of amino acids were identified in BMF (Table 3). Following fermentation, 3 types of organic acids were detected in BMF, with a total content of

approximately 0.7%. Furthermore, BMF contains 0.68% phospholipids, 3 types of nucleotides, 5 types of minerals, and 11 types of vitamins. After fermentation by Bifidobacterium adolescentis, the content of protein and lactose in milk decreased, while the content of galactose, glucose, and GABA increased as shown in Table 4.

Table 3. The composition of BMF

Category	No.	Test Item	Content/%
Total Sugar	1	Total Sugar Content	2.38
Monosaccharides and free sugars	1	Glucose	0.32
	2	Galactose	0.14
	3	Glucosamine	0.024886
	4	Trehalose	0.011478
	5	Galactosamine	0.009578
	6	Trehalose Acid	0.008874
	7	Fucose	0.003832
	8	Rhamnose	0.00301
	9	Xylose	0.00209
	10	Arabinose	0.002007
	11	Gluconic Acid	0.001613
	12	Lactose	1.74
	13	Maltose	0.04
Proteins	1	Total Protein	0.21
	2	A total of 121 types of proteins, 109 peptides	
Amino Acids	1	γ-Aminobutyric Acid	0.001875
	2	Alanine	0.000682
	3	Aspartic Acid	0.00022
	4	Glutamic Acid	0.000203
	5	Glycine	0.000143
	6	Proline	0.00008
	7	Serine	0.000049
	Total	/	0.003638
Organic Acids	1	Acetic Acid	0.305717
	2	Citric Acid	0.211283
	3	Lactic Acid	0.181471
	Total	/	0.698471
Phospholipids	1	Total Phospholipids	0.6844
Nucleotides	1	Sphingosine	0.000251
	2	Uridine	0.000194
	3	Cytidine	0.000092
	Total	/	0.000537
Minerals	1	Potassium (K)	0.0604
	2	Calcium (Ca)	0.0452
	3	Sodium (Na)	0.0429

	4	Phosphorus (P)	0.0282
	5	Magnesium (Mg)	0.00453
	Total	/	0.18123
Vitamins	1	Pantothenic Acid	0.001128146
	2	Vitamin B2	0.000033613
	3	Vitamin B1	0.000025353
	4	Vitamin B6	0.000017301
	5	Niacin	0.000008921
	6	Folic Acid	0.000008524
	7	Pyridoxine HCl	0.000003703
	8	Pyridoxal Phosphate	0.000001343
	9	Vitamin D2	0.000005121
	10	Vitamin E	0.00000193
	11	Vitamin D3	0.000001516
	Total	/	0.001235471

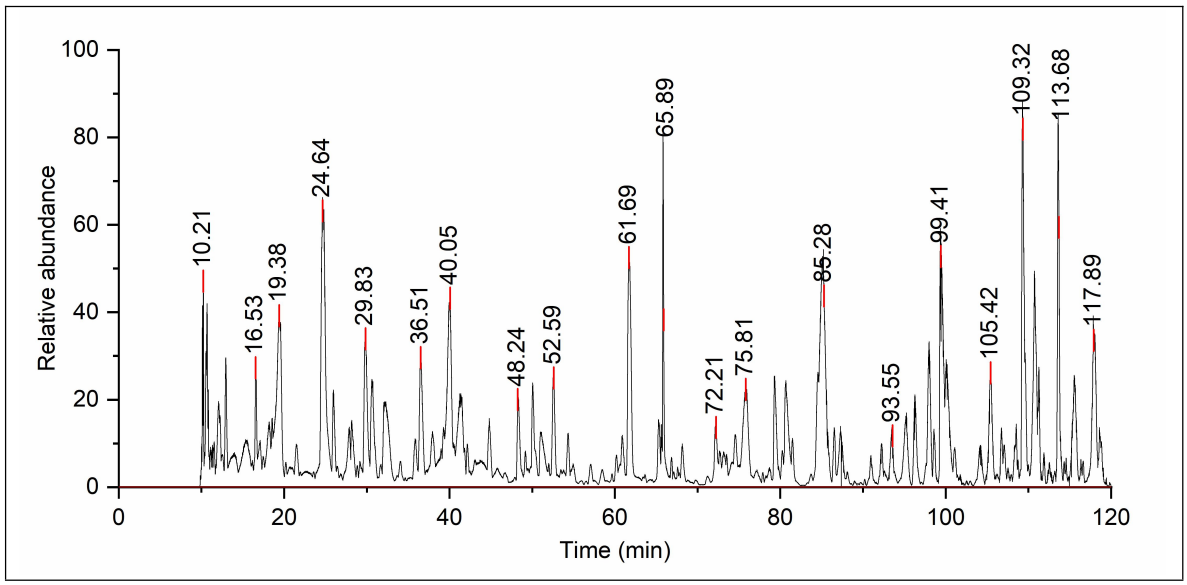

Figure 1. Total ion chromatogram (TIC) for the analysis of protein and peptide.

Table 4. Comparison of Components Content Before and After Fermentation.

Component	Before Fermentation/%	After Fermentation/%
Protein	9.37	2.01
Lactose	2.58	1.74
Galactose	0	0.14
Glucose	0.03	0.32
γ-Aminobutyric Acid	0	0.119

3.2. Effect of BMF on DNA Damage in 3T3 Cells Stimulated with H_2O_2

Exposure to hydrogen peroxide (H_2O_2) induces DNA damage, often resulting in double-strand breaks. In response, the serine residue at position 139 (Ser-139) of the H2AX protein undergoes rapid and extensive phosphorylation. This phosphorylated variant of H2AX is termed γH2AX [17]. Upon stimulation with H_2O_2, the positivity rate of γH2AX is significantly elevated (Figure 2). However, in cells treated with BMF, this positivity rate is markedly reduced. Specifically, the group treated with 1% BMF shows a 34% reduction in γH2AX positivity compared to the model group. These findings indicate that BMF effectively mitigates oxidative stress damage induced by H_2O_2, offering a protective effect on DNA.

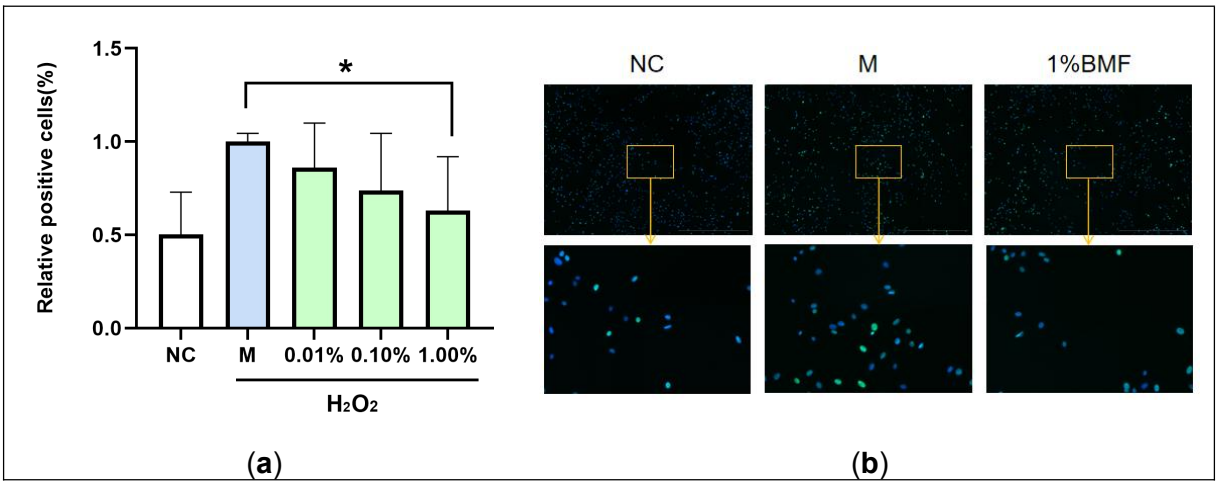

Figure 2. Results of DNA damage protection experiments. (a) Statistical results of relative positivity rate of γ H2AX; (b) Cell staining image.

3.3. Effect of BMF on TNF-α and IL-1β Gene Expression by THP-1 Cells Stimulated with LPS

Compared with the normal cells in the negative control group (NC), the expression levels of the inflammatory cytokines TNF-α and IL-1β were significantly elevated in the model group stimulated with LPS. However, treatment with 1% BMF markedly reduced the expression of these cytokines, with TNF-α decreasing by 29.6% and IL-1β by 9.2% compared to the model group as shown in Figure 3. These results suggest that BMF effectively alleviates LPS-induced inflammation in THP-1 cells.

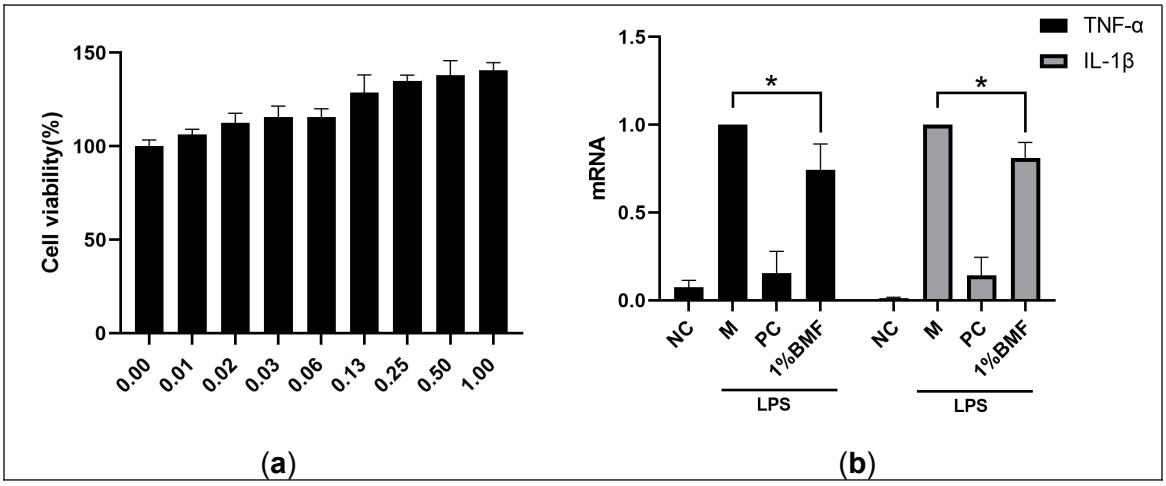

Figure 3. Anti-inflammatory effects in THP-1 cells. (a) Determination of the safe concentration of BMF in THP-1 cells, (b) Expression levels of TNF-α and IL-1β following LPS stimulation and BMF treatment.

3.4. Effect of BMF on Reducing Lipofuscin in Caenorhabditis elegans

Compared with the control group, C. elegans treated with 10% BMF showed a significant reduction of 13.79% in lipofuscin fluorescence intensity and a clear dose dependence as shown in Figure 4. These results indicate that BMF effectively inhibits the production and accumulation of lipofuscin.

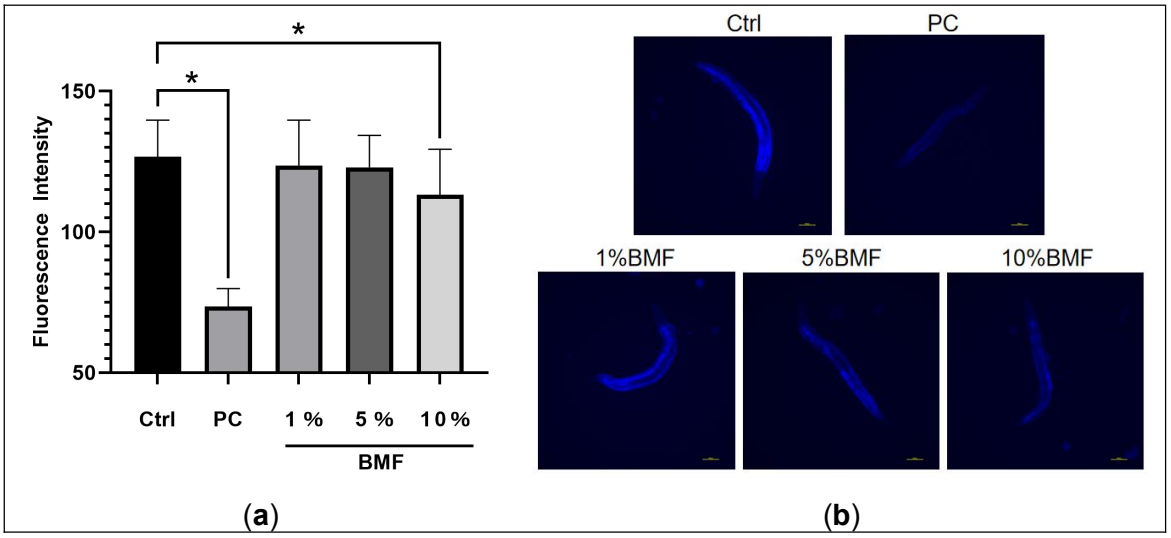

Figure 4. Lipofuscin analysis in Caenorhabditis elegans. (a) Quantitative analysis of lipofuscin fluorescence intensity in C. elegans, (b) Fluorescence microscopy images of lipofuscin accumulation in C. Elegans.

3.5. Effect of BMF on Tyrosinase Activity

BMF demonstrates the capacity to inhibit tyrosinase, with the inhibitory rate of this enzyme increasing in a concentration-dependent manner as the concentration of BMF rises (Table 5). This finding suggests that BMF has significant potential to impede melanin formation.

Table 5. Tyrosinase inhibition rate

BMF concentration(%)	Tyrosinase inhibition rate(%)	SD
100	43.11	0.71
50	25.98	1.33
20	7.10	1.10

3.6. Effect of BMF on Hydroxyl Radical Scavenging Ability

At a BMF concentration of 3.1%, the hydroxyl radicals scavenging rate exceeded 50% (Figure 5). When the concentration increased to over 25%, the scavenging rate surpassed 90%, reaching a peak value of 92.8%. These results suggest that at higher concentrations, BMF effectively eliminates the majority of hydroxyl radicals in the system, demonstrating a strong antioxidant capacity.

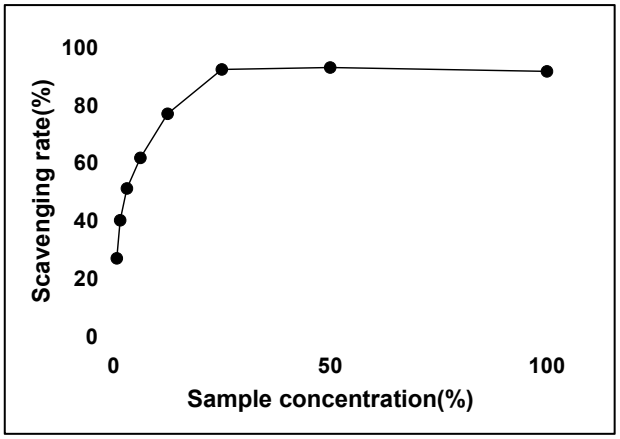

Figure 5. Hydroxyl radical scavenging activity of BMF.

3.7. Effect of BMF on Reducing Skin Erythema

Following tape stripping on the inner forearm, the erythema index (EI) significantly increased. Topical application of 10% BMF led to a marked reduction in EI, showing an improvement rate of 36.65% after 2 hours (Figure 6). Compared to the control group (NC), the BMF-treated group demonstrated consistently greater improvements, with EI reduction rates 9.25%, 12.98%, and 15.10% higher than those of the control group at 0.5, 1, and 2 hours post-application, respectively. These findings indicate that BMF exhibits a significant soothing effect on skin erythema induced by irritation.

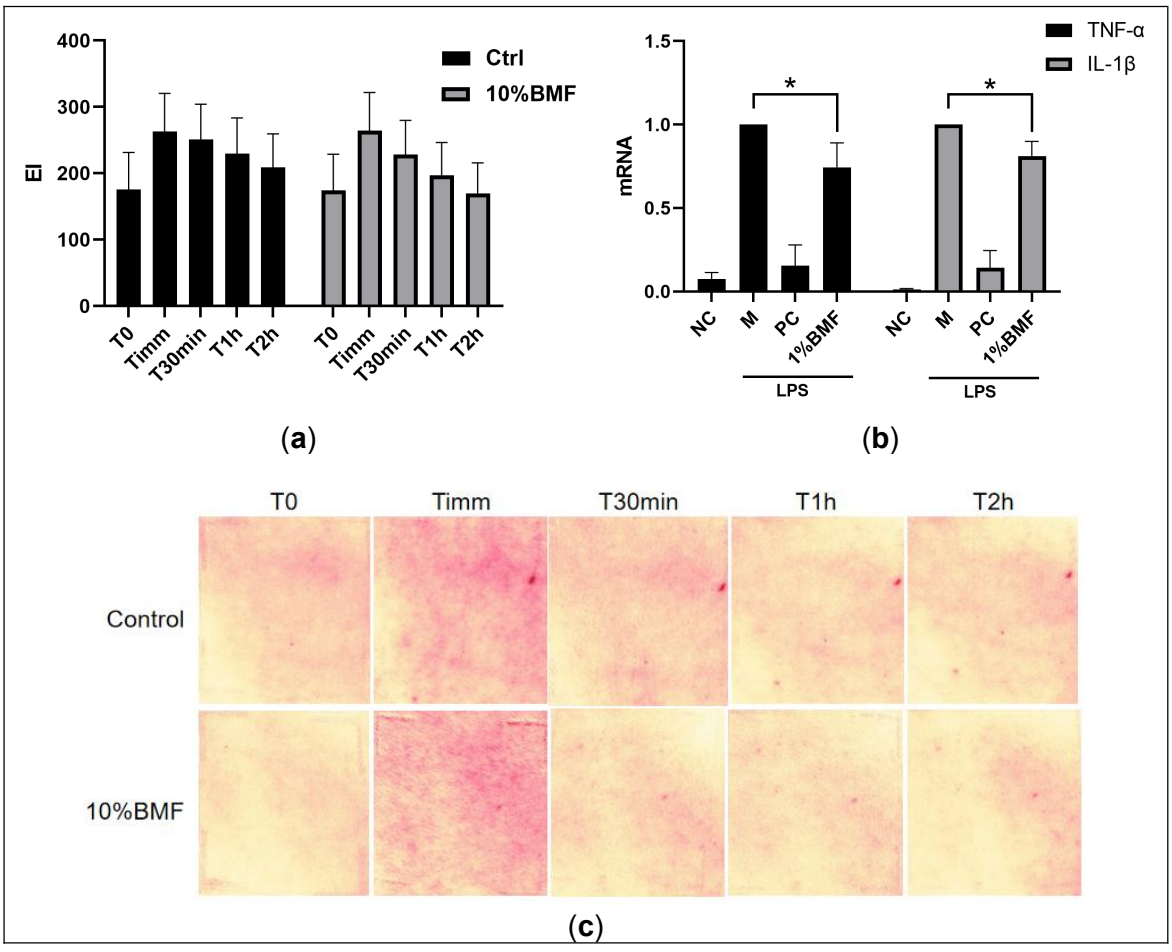

Figure 6. Erythema index assay. (a)EI, (b) EI recovery rate, (c) Representative photographs of the tested skin areas.

4. Discussion

A very systematic full composition analysis of BMF has been conducted in this study. Fermentation of milk by Bifidobacterium adolescentis leads to the breakdown of proteins into smaller peptides and amino acids, while lactose is hydrolyzed into galactose and glucose—components that are more readily absorbed by the skin. Simultaneously, the fermentation process produces organic acids and other bioactive compounds that contribute to the renewal of keratinocytes. The resulting BMF is enriched with a broad spectrum of bioactive constituents, including sugars, proteins, peptides, amino acids, GABA, lipids, organic acids, vitamins, nucleotides, and minerals. These components may act synergistically to promote a more even skin tone and reduce hyperpigmentation, as illustrated in Figure 7.

Both in vitro and clinical studies support the skin-tone-evening effects of BMF. Using cellular models, C. elegans, and human subjects, BMF has demonstrated comprehensive efficacy by targeting interconnected pathways such as oxidative stress, inflammation, lipofuscin accumulation, and melanogenesis—offering a multifaceted approach that outperforms conventional single-target treatments. BMF inhibited tyrosinase activity by 43.1%, while also exerting significant anti-inflammatory effects, as evidenced by reductions in TNF-α (29.6%, $p \leq 0.05$) and IL-1β (9.2%, $p \leq 0.05$). It also exhibited a strong hydroxyl radical scavenging capacity (91.5%) and decreased lipofuscin accumulation by 13.8% ($n = 30$, $p < 0.05$). In a 4-week clinical trial, topical application of BMF resulted in a 15.1% improvement in skin tone compared to the control group ($n = 30$, $p \leq 0.0001$), reflecting reduced redness and improved skin uniformity.

Nevertheless, further investigation is warranted to identify the key components within the fermented product that contribute to skin tone modulation, as well as to elucidate their synergistic mechanisms. Clarifying the regulatory network by which BMF influences pigmentation and inflammation will enhance our understanding of its dermocosmetic potential.

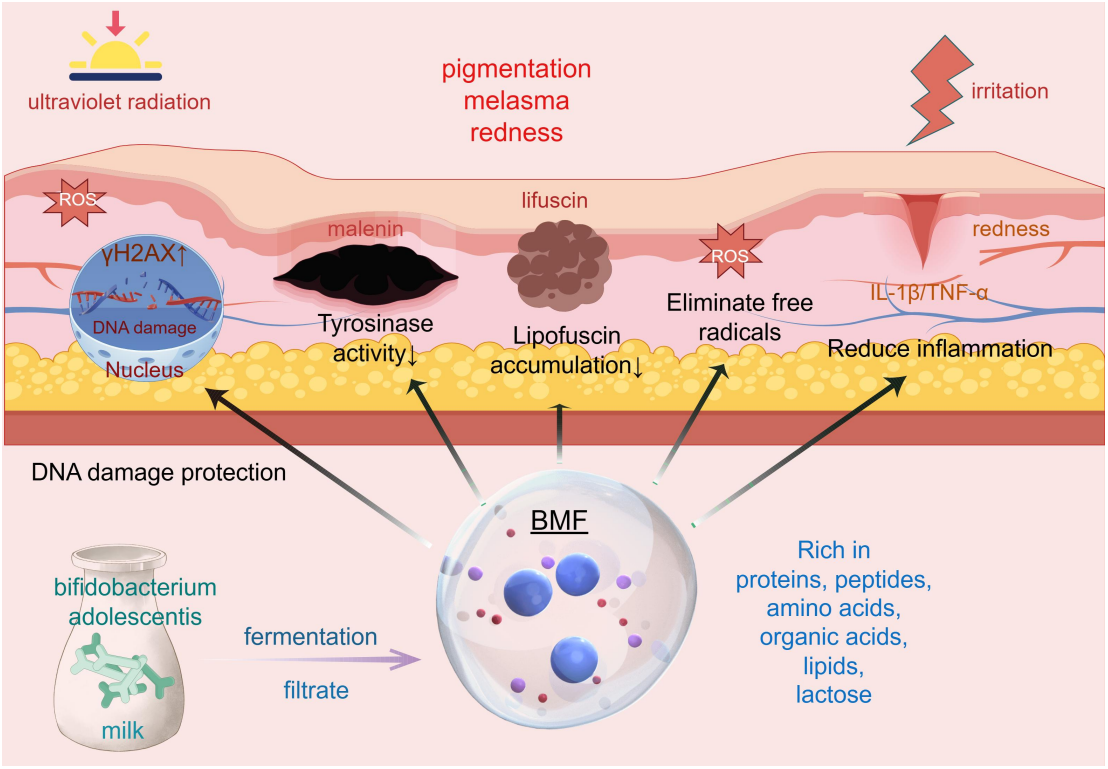

Figure 7. Schematic representation of the mechanism underlying the skin tone-evening effect of BMF.

5. Conclusion

This study demonstrates that BMF provides an innovative solution for the multi-dimensional improvement of uneven skin pigmentation by synergistically regulating lipofuscin accumulation, inflammatory responses, and melanin synthesis pathways. The combined effects of its tyrosinase inhibitory activity, reduction in lipofuscin accumulation, and improvement in clinical erythema index contribute to the alleviation of skin redness, yellowing, age and dark spots, and hyperpigmentation, clearly outperforming traditional single-target ingredients such as hydroquinone or vitamin C. Its ability to neutralize free radicals and protect against oxidative damage makes it a promising solution for sensitive skin. As part of a skincare routine, BMF could act as a "Skin's Aurora Palette," addressing multiple skin discolorations and promoting a luminous, even complexion. Future research could incorporate AI-driven formulation optimization to explore the synergistic potential of BMF in combination with sunscreens or barrier-repair ingredients, advancing the development of 'precision skincare' technologies.

6. References

[1] Chen, J., Liu, Y., Zhao, Z., & Qiu, J. (2021). Oxidative stress in the skin: Impact and related protection. International Journal of Cosmetic Science, 43(5), 495-509.
[2] Serre, C., Busuttil, V., & Botto, J. M. (2018). Intrinsic and extrinsic regulation of human skin melanogenesis and pigmentation. International journal of cosmetic science, 40(4), 328-347.
[3] Jung, T., Bader, N., & Grune, T. (2007). Lipofuscin: formation, distribution, and metabolic consequences. Annals of the New York Academy of Sciences, 1119(1), 97-111.

[4] Sofen, B., Prado, G., & Emer, J. (2016). Melasma and post inflammatory hyperpigmentation: management update and expert opinion. Skin therapy letter, 21(1), 1-7..
[5] Chen, S., Chen, L., Qi, Y., Xu, J., Ge, Q., Fan, Y., ... & Wang, L. (2021). Bifidobacterium adolescentis regulates catalase activity and host metabolism and improves healthspan and lifespan in multiple species. Nature Aging, 1(11), 991-1001.
[6] Jena, R., & Choudhury, P. K. (2023). Bifidobacteria in fermented dairy foods: A health beneficial outlook. *Probiotics and Antimicrobial Proteins*, 1-22.
[7] Sun, Y., Guo, S., Kwok, L. Y., Sun, Z., Wang, J., & Zhang, H. (2024). Probiotic Bifidobacterium animalis ssp. lactis Probio-M8 improves the fermentation and probiotic properties of fermented milk. *Journal of Dairy Science*, *107*(9), 6643-6657.
[8]Chen, Y., Li, P., Huang, W., Yang, N., Zhang, X., Cai, K., ... & Liao, Q. (2025). Structural characterization and immunomodulatory activity of an exopolysaccharide isolated from Bifidobacterium adolescentis. International Journal of Biological Macromolecules, 140747.
[9] Li, B., Wang, H., Wang, M., Liang, H., Hu, T., Yang, J., ... & Sun, Y. (2025). Genome analysis of Bifidobacterium adolescentis and investigation of its effects on inflammation and intestinal barrier function. *Frontiers in Microbiology*, *15*, 1496280.
[10] Krivorotova, T., & Sereikaite, J. (2014). Determination of fructan exohydrolase activity in the crude extracts of plants. *Electronic Journal of Biotechnology*, *17*(6), 329-333.
[11] Euber, J. R., and J. R. Brunner. "Determination of lactose in milk products by high-performance liquid chromatography." *Journal of Dairy Science* 62.5 (1979): 685-690.
[12] Ramani, Akshay, et al. "Development and validation of a HPLC-UV method for the quantification of major phospholipids in milk." *Journal of Food Composition and Analysis* 134 (2024): 106552.
[13] Contreras-Sanz, Alberto, et al. "Simultaneous quantification of 12 different nucleotides and nucleosides released from renal epithelium and in human urine samples using ion-pair reversed-phase HPLC." *Purinergic signalling* 8 (2012): 741-751.
[14] Park, C., Lee, H., **, S., Park, J. H., Han, M. H., Jeong, J. W., ... & Choi, Y. H. (2022). The preventive effect of loganin on oxidative stress-induced cellular damage in human keratinocyte HaCaT cells. BioScience Trends, 16(4), 291-300.
[15] Chanput, W., Mes, J., Vreeburg, R. A., Savelkoul, H. F., & Wichers, H. J. (2010). Transcription profiles of LPS-stimulated THP-1 monocytes and macrophages: a tool to study inflammation modulating effects of food-derived compounds. *Food & function*, *1*(3), 254-261.
[16] Di Petrillo, A., González-Paramás, A. M., Era, B., Medda, R., Pintus, F., Santos-Buelga, C., & Fais, A. (2016). Tyrosinase inhibition and antioxidant properties of Asphodelus microcarpus extracts. *BMC complementary and alternative medicine*, *16*, 1-9.
[17] Mah, L. J., El-Osta, A., & Karagiannis, T. C. (2010). γH2AX: a sensitive molecular marker of DNA damage and repair. Leukemia, 24(4), 679-686.